VOL. 9, NO. 3, MARCH 2014 ISSN 1819-6608
ARPN Journal of Engineering and Applied Sciences

www.arpnjournals.com

SAFETY ASSESSMENT OF A LIGHT TRANSPORT AIRCRAFT (LTA) IN THE EVENT OF UNCONTAINED ROTOR BURST AND PROPELLER BLADE FAILURE

Rashmi Hundekari and Abbani Rinku
CSIR-National Aerospace Laboratories, Bangalore, India
E-Mail: rashmi@nal.res.in

ABSTRACT

Throughout the life cycle of an aircraft, it is likely that it may encounter an uncontained engine rotor or propeller blade failure due to probable malfunction or failure of single or multiple engine components, inadequate rotor and casing design, fatigue, material imperfections, assembly errors and foreign object ingestion. Uncontained engine rotor or propeller blade failure can lead to catastrophic failure if not addressed adequately during design. To ensure safety of the flight in the event of rotor burst or propeller blade failure federal aviation regulations has set forth compliance requirements (FAR sections 25.903, 25.905.d) which states that the airplane must be capable of successfully completing a flight during which likely structural damage occurs as a result of a propeller blade impact, uncontained fan blade impact, uncontained engine rotor failure or uncontained high energy rotating machinery failure. Aircraft manufactures has to comply with the safety requirements mentioned above. Hence it is required to assess the risk, take adequate design measures to minimize the risk and show compliance by analysis or test that the damage caused is minimal and aircraft is capable of completing safe flight in the event of uncontained rotor failure. This paper demonstrates the methodology to be followed for performing safety assessment of a typical light transport aircraft (LTA) in the event of an uncontained rotor burst and propeller blade failure. Assessment method presented in this paper is generic in nature and can be used to assess the safety of any class of transport aircraft.

Keywords: uncontained engine failure, safety assessment, threat window, high speed impact, post impact analysis, functional hazards.

INTRODUCTION

Safety of the flight is a prime concern in aviation industry. Accidental damage and engine rotor failures have caused many catastrophes in aviation history. To avoid catastrophe and ensure safe flight as per Federal aviation regulation (FAR-Section 25.903, 25.905.d) for aircraft manufacturer it is mandatory to take adequate design precautions and minimize the hazards to the airplane in the event of an engine rotor failure. This paper in detail describes the methodology laid down to comply with uncontained rotor burst and propeller blade failure requirements. A detailed step by step safety assessment has been carried out for a typical light transport aircraft (LTA). Safety assessment includes, establishing release path for engine rotors and propeller blades, identification of impact areas, identification of critical structural components and systems falling within these impact zones, carrying out the detailed functional hazard analysis. Performing high speed impact and post impact analysis to assess the extent of structural damage. The high speed impact and post impact analysis has been carried out using commercially available finite element code “ABAQUS” and the overall structural integrity in the event of uncontained rotor burst has been checked. Post impact behavior has been assessed. Propeller blade off post impact analysis results revealed that in presence of impact damage also, the aircraft stiffened panels are capable of withstanding flight loads.

RELEASE PATH FOR ENGINE ROTOR AND PROPELLER BLADE

LTA under consideration is powered by 2 turboprop engines. This engine consist of engine rotors (2 turbine rotors, 1 impeller, 5 compressor rotors) and a propeller and are stationed as shown in Figure-1. As per the guidelines given in advisory circular AMC20-128A it has been assumed that release of engine rotor or propeller blade fragment can happen from any clock position of the rotor and from any one engine at one point of time. For different clock positions, release paths have been established and threat windows are identified. In case of engine rotors, disc fragment travels along a trajectory that is tangential to the sector centroid locus, in the direction of rotor rotation. Release path for rotors has been shown in Figure-2. For propeller blade release path involute trajectory has been defined and it is as shown in Figure-3. The fragment of rotor and propeller is considered to possess infinite energy and therefore are capable of severing lines, wiring, cables and unprotected structure in its path and to be un-deflected from its original trajectory unless deflection shields are fitted.

VOL. 9, NO. 3, MARCH 2014 ISSN 1819-6608
ARPN Journal of Engineering and Applied Sciences

www.arpnjournals.com

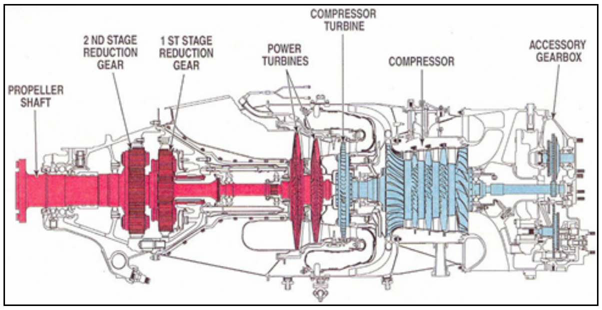

Figure-1. Turboprop engine with various rotors, courtesy Pratt and Whitney.

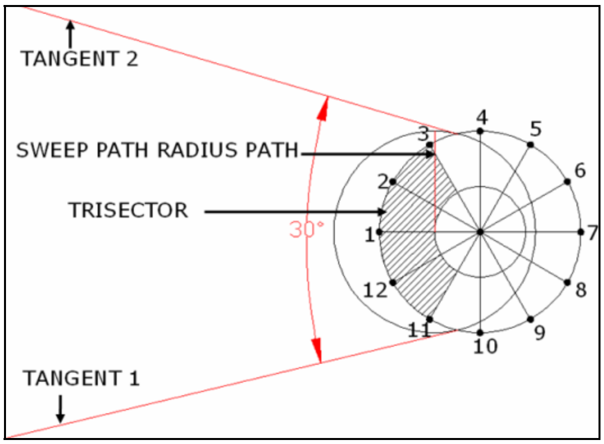

Figure-2. Release path for engine rotor fragment when released from rotor clock position '1'.

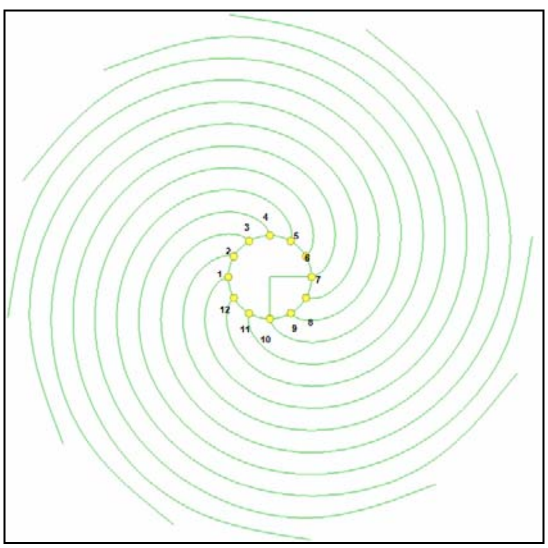

Figure-3. Release paths for propeller blade.

UNCONTAINED ENGINE ROTOR AND PROPELLER BLADE IMPACT AREAS (THREAT WINDOWS)

After establishing release path for rotor and propeller blade, zones where they are likely to impact the aircraft structure (impact zones) such as nacelle, stub-wing, fuselage, and empennage have been plotted and corresponding threat windows have been identified. Threat window obtained for small rotor fragment with $\pm 15^0$ spread angle is as shown in Figure-4.

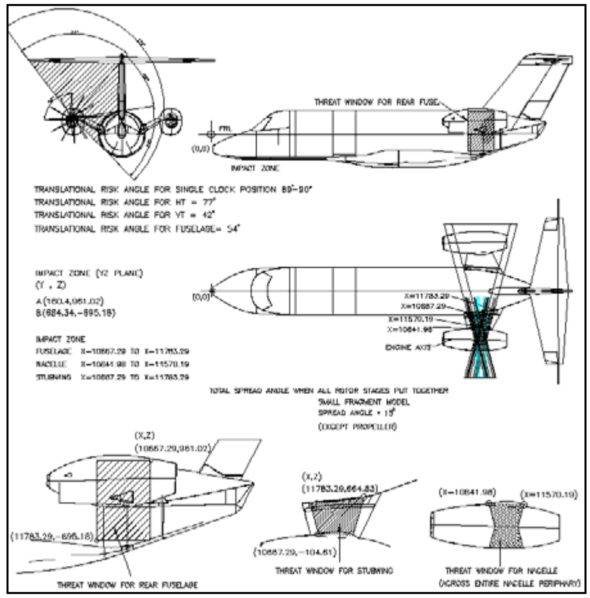

Figure-4. Threat window for engine rotor failure.

Spread of the threat window for uncontained engine rotor failure is as mentioned in Figure-4 Propeller blade off is more severe than engine rotor failure as blade is directly exposed to the empennage. Hence the analysis pertaining to propeller blade off condition is presented in this paper. Threat window for propeller blade release is shown in Figure-5. Spread for threat window of propeller blade is as mentioned at Figure-5.

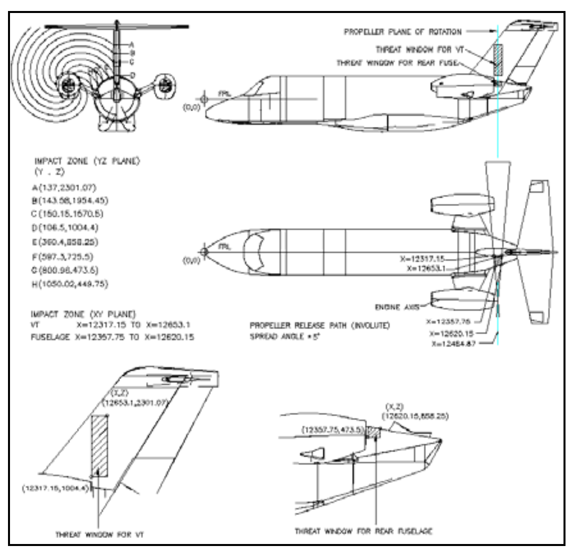

Figure-5. Threat window for propeller blade failure.

ARPN Journal of Engineering and Applied Sciences

STRUCTURAL SAFETY ASSESSMENT

High speed impact and post impact analysis has been carried out for part of rear fuselage assembly which is likely to get impacted by the propeller blade fragment. Extent of structural damage has been assessed and to this damaged structure in flight panel loads obtained from global shell analysis for critical load case have been applied. Structural integrity has been checked. These post impact studies has provided insight into post impact behavior of the rear fuselage stiffened panel. Abaqus explicit solver has been used for nonlinear finite element analysis. Johnson Cook material model is used for simulating impact on stiffened rear fuselage panel. Methodology followed is same as that described and validated in literature (Murat Buyuk *et al*., 2009)

JOHNSON COOK (J-C) MATERIAL MODEL

Propeller blade release is a high speed impact scenario and high strain rates are expected to occur during impact hence strain rate and temperature dependent viscoplastic J-C material model has been selected for accurate damage prediction. J-C model is a validated material model and has been used by many researchers to simulate uncontained engine rotor failure and its effect on aircraft structure. Various material parameters used during explicit analysis are as listed in table: 1 and can be found in the literature (Kay *et al*., 2007). J-C model calculates flow stress using equation (1)

$$\sigma_Y = (A+B\ \varepsilon^n)\ (1+ C \ln \acute{\varepsilon}^*)\ (1-T^{*m}) \quad (1)$$

Where

σ_Y = effective stress; ε = effective plastic strain
ε^* = normalized effective plastic strain rate
n = work hardening exponent
A, B, C and m = material constants and there description has been given in Table-1

$$T^* = (T-T_{room})/ (T_{melt}- T_{room}) \quad (2)$$

Where

T_{room}= Room temperature; T_{melt} = Melting temperature

In equation (1) it has been assumed that percentage of plastic work done during deformation produces heat while deforming the material, based on this corresponding rise in temperature corresponding temperature dependent response of the panel has been obtained. Johnson Cook Damage initiation criterion for ductile material has been used to predict the damage initiation according to this criterion damage initiates when the effective plastic strain (ε_p) at given time interval, at any point in the material is equal to or greater than the equivalent plastic strain at onset of damage ($\acute{\varepsilon}_p$); beyond this point damage evolves as per the damage evolution law given by equation (3) and the final failure occurs when the damage variable (D) becomes one. Equivalent plastic strain at onset of damage has been calculated as per equation (3).

$$\acute{\varepsilon}_p = [D_1+ D_2\exp(D_3\sigma^*)][1+D_4\ln(\acute{\varepsilon}^{pl}/\acute{\varepsilon}_0)][1+D_5T^*] \quad (3)$$

Where

D_1-D_5 are failure parameters
σ^* = mean stress normalized by the effective stress
$\acute{\varepsilon}^{pl}$ = plastic strain rate, $\acute{\varepsilon}_0$ = reference strain rate
Damage evolution law used is given by equation (4)

$$D = \sum \Delta\varepsilon_p/ \acute{\varepsilon}_p \quad (4)$$

Where

$\acute{\varepsilon}_p$ = equivalent plastic strain at onset of damage
$\Delta\varepsilon_p$ = increment in effective plastic strain during an increment in loading
D = damage variable

When damage variable (D) reaches a value of 1 total loss of stiffness occurs leading to total loss of load carrying capability and the elements gets deleted from the finite element model, simulating loss of material from the concerned zone.

Table-1. J-C material model parameters for Al- 2024-T3.

Material	Al 2024 T3	
Material parameter	**Notation**	
Density (ρ) [kg/m^3]	ρ	2770
Modulus of elasticity [MPa]	E	73084
Poisson's ratio	ν	0.33
Static Yield Limit [MPa]	A	369
Strain hardening modulus [MPa]	B	684
Strain hardening exponent	n	0.73
Strain rate coefficient	C	0.0083
Thermal softening exponent	m	1.7
Reference strain rate	s^{-1}	1
Reference temperature [^{0}K]	T_{room}	294
Melting temperature [^{0}K]	T_{melt}	775
Specific heat [J/kg ^{0}K]	c_p	875
Damage parameters	D_1	0.31
	D_2	0.045
	D_3	-1.7
	D_4	0.005
	D_5	0

J-C Material parameters used for simulating high speed impact on Al2024-T3 stiffened panel are given in Table-1

VOL. 9, NO. 3, MARCH 2014 ISSN 1819-6608
ARPN Journal of Engineering and Applied Sciences

www.arpnjournals.com

STIFFENED REAR FUSELAGE PANEL GEOMETRY

Part of rear fuselage structure which is falling within propeller blade release impact zone has been considered for high speed impact analysis. This fuselage shell is of semi-monocoque construction with sheet metal skin stiffened by the stringers longitudinally and with frames (bulkhead) in transverse direction. The panel size is selected in such a way that it will simulate the overall structure. Stiffened panel size is 700 mm x 525 mm with 8 stringers and two frames. Skin, stringers are 1.2 thick and frame top flange is 2.5 mm thick. For stiffened rear fuselage, for simulating damage initiation and evolution, material parameters mentioned in Table-1 are used.

PROPELLER FRAGMENT GEOMETRY

Propeller fragment which is impacting on the stiffened panel is assumed to be a rigid impactor. Discrete rigid part definition available in ABAQUS has been used for simulation of the propeller fragment. One fourth of the blade fragment from the tip has been considered for modelling. Propeller specification is MTV-27-2-N-C-F-R (P) with 2.65m diameter and is rotating at 1700 RPM speed for max and continuous power rating of 1200 SHP. In the event of blade off it follows an involute path and impacts the rear fuselage stiffened panel with the speed of 228 m/s. The mass of the fragment is 1.5 kg. The impact energy is of 39 MJ. These energy levels are close to the ballistic impact scenario.

STIFFENED REAR FUSELAGE PANEL AND PROPELLER FINITE ELEMENT MODEL

Stiffened rear fuselage panel is modeled using continuum shell element (SC8R) with 3 DOF per node and using reduced integration method. Minimal 3 elements through the thickness are being used. Figures 6(a) and 6(b) shows the top face and bottom face of rear fuselage stiffened panel meshed model. Figure 6(c) depicts the propeller (projectile) and rear fuselage stiffened panel (target) impact model.

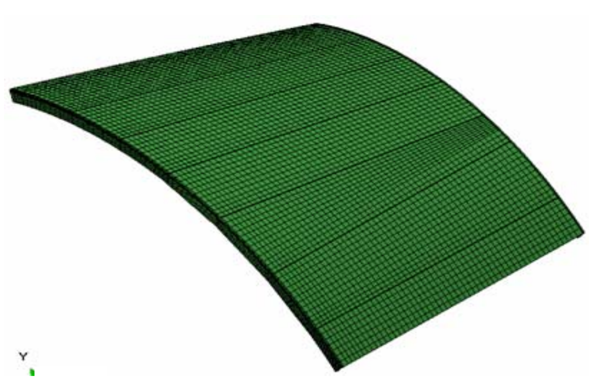

Figure-6(a). Meshed model - top face-stiffened rear fuselage panel.

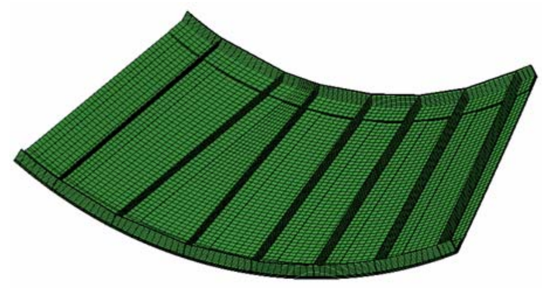

Figure-6(b). Meshed model-bottom face-stiffened rear fuselage panel.

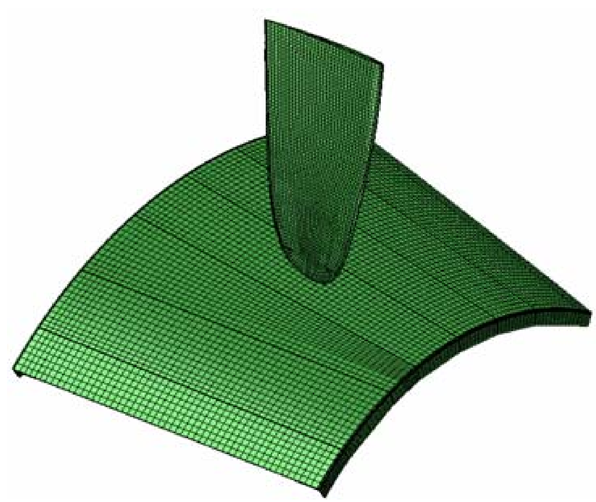

Figure-6(c). Propeller fragment and rear fuselage stiffened impact model.

HIGH SPEED DYNAMIC IMPACT ANALYSIS RESULTS

Results of high speed impact analysis show a petal formation and sever buckling of panel along with shell bending. Material has been lost from the area beneath the fragment. Figure-7(a) and 7(b) depicts the top and bottom face of damaged rear fuselage panel. Vonmises stress distribution plot at top and bottom face of the stiffened panel is shown in Figure- 8(a) and Figure-8(b), respectively.

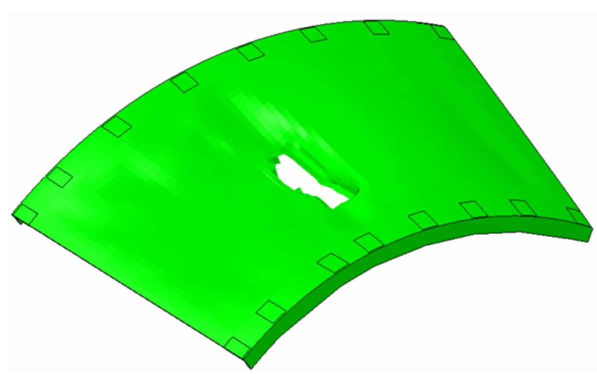

Figure-7(a). Top face - rear fuselage damaged panel.

VOL. 9, NO. 3, MARCH 2014 ISSN 1819-6608
ARPN Journal of Engineering and Applied Sciences

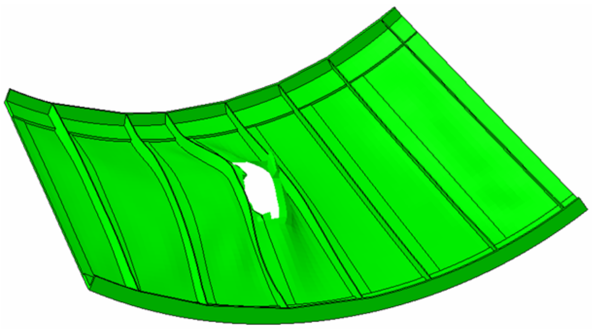

Figure-7(b). Bottom face - rear fuselage damaged panel.

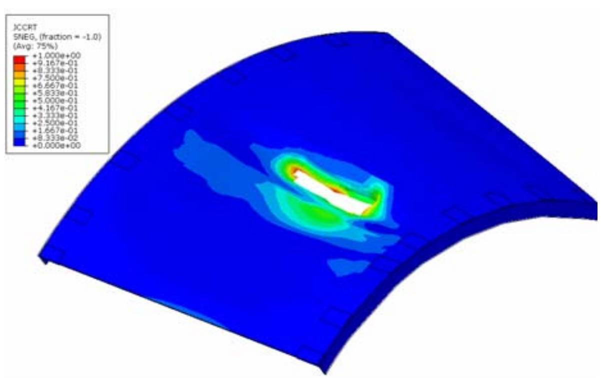

Figure-8(a). J-C damage criterion plot-top face - rear fuselage damaged panel.

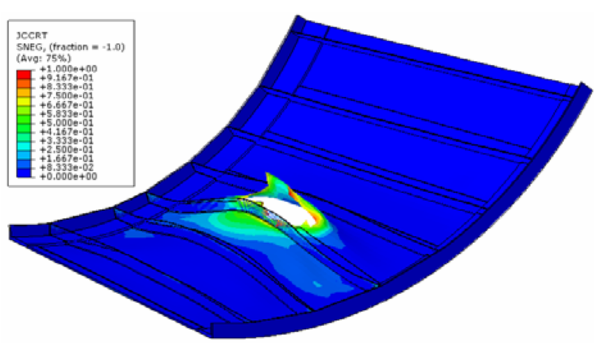

Figure-8(b). J-C damage criterion plot -Bottom face - rear fuselage damaged panel.

POST IMPACT ANALYSIS RESULTS

Damaged rear fuselage panel has been imported and subjected to the panel loads to check whether the structure is capable of supporting the flight loads in presence of this impact damage. FE analysis has been carried out and from post impact simulation results it has been observed that when the panel loads obtained from the global analysis of the entire fuselage are applied to the damaged panel; stress levels observed are well within material allowable, near damaged area local stress concentration has been observed. Vonmises stress level near the vicinity of damage is 400MPa where as in adjacent panel it is observed to be in 300 to 260 MPa. Redistribution of the panel loads has been taken place and stress levels observed in adjacent panels are higher than the stress levels observed for original undamaged panel.

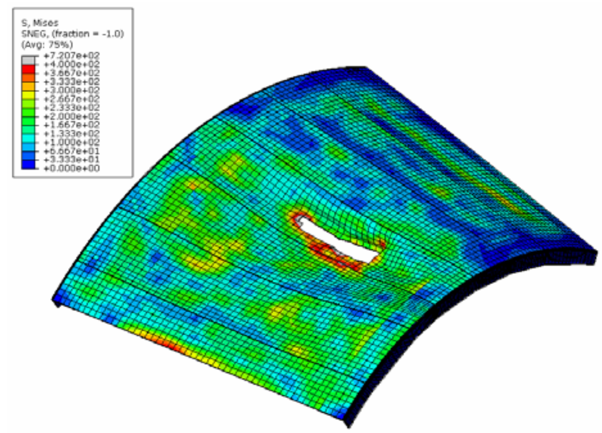

Figure-9. Vonmises stress plot post impact analysis.

FUNCTIONAL HAZARD

From high speed impact analysis results it is evident that the blade will penetrate the rear fuselage panel. Though the fragment will lose small of amount energy but still possesses residual energy high enough to further penetrate some other adjacent structural member and continue damaging the structure and aircraft system components coming in the path, damage is likely to continue till the fragment loses it's all the energy or escapes out of rear fuselage. Keeping this possibility in view for threat windows identified for uncontained engine rotor failure and propeller blade release conditions are superimposed on aircraft systems and airframe to study the structural and system failures. Further detailed functional hazard assessment has been conducted for all the aircraft systems based on the assessment appropriate design precautions have been taken to complete the safe flight in the event of uncontained rotor failure. Functional hazard data has been not included in the paper as it is a classified data.

CONCLUSIONS

Uncontained engine rotor failure and propeller blade release cause severe damage to aircraft structure and to its systems leading to catastrophic failure of the aircraft. To prevent this catastrophe aircraft designer has to take adequate design precautions. It is required to identify the threat windows well in advance and locate the principal structural elements and important system components away from the threat window. This paper presents a methodology for the safety assessment of an aircraft in the event of engine rotor or propeller blade failure for a typical LTA. A detailed high speed impact analysis has been performed and the extent of damage to the airframe is predicted. The impact analysis shows a complete penetration of the panel. Damaged rear fuselage model showed petaling, panel buckling and bending. With damage in place post impact analysis has been carried out by imposing global load effects on the panel. From the post impact response of the panel, it is evident that in the presence of impact damage the airframe is still capable of withstanding critical flight loads. Outcome of the study resulted in taking up some appropriate design precautions by re-locating/re-designing few of the flight critical components Methodology laid down is generic in nature and can be followed for all class of aircrafts.

TERMINOLOGY USED

Rotor

Components of the engine that analysis/test or experience has shown can be released during uncontained failure.

Uncontained failure

Any failure that results in the release of fragments from the rotor.

Critical components

Any component whose failure would contribute to or cause a failure condition that would prevent the continued safe flight and landing of the airplane. These components should be considered individually and in relation to other components that could be damaged by the same or by other fragments from the same uncontained event.

Fragment spread angle

The angle measured fore and aft from the rotor plane of rotation as inscribed by the blade axis as it rotates about its shaft centerline.

Impact area

The area of the airplane likely to be impacted by uncontained fragments generated in the event of a failed rotor blade.

Propeller blade

The complete blade from the airfoil surface to the retention and pitch change portion of the blade that may be contained within the hub. Included are all components attached to the blade such as counter weights, clamps, erosion shields, cuffs, de-ice boots, and hub assemble.

REFERENCES

AMC20-128A, “Advisory circular”, U.S. department of Transportation, Federal aviation administration, 1999.

Part 25: Airworthiness Standards: Transport Category.

Johnson G. R., and Cook W. H., “A constitutive model and data for metals subject to large strains, high strain rates and high temperatures”, Proc. 7th Int. Symp. on Ballistics, The Hague, The Netherlands, 541–547, 1983.

Kay G., Goto D., and Couch R., “Statistical testing of aluminum, titanium, lexan and composites for transport airplane rotor burst fragment shielding”, FAA Rep.No. DOT/FAA/AR-07/26, Federal Aviation Administration, Washington, D.C, 2007.

Murat Buyuk, Steve Kan, Matti J., J Loikkanen, “Explicit finite element analysis of 2024-T3/T351 aluminum material under impact loading for airplane engine containment and fragment shielding”, Journal of Aerospace Eng., 287- 295, 2009.